Strange kinetics

Michael F. Shlesinger, George M. Zaslavsky & Joseph Klafter

The once abstract notions of fractal space and time now appear naturally and inevitably in chaotic dynamical systems and lead to 'strange kinetics' and anomalous transport properties. An understanding of this kind of dynamical behaviour should provide insights into, for example, turbulent fluid dynamics and particle random-walk processes.

IT is now widely appreciated that complex, seemingly random behaviour can be governed by deterministic nonlinear equations. Such complex deterministic behaviour has been termed chaotic. But rather than being a harbinger of the demise of random processes, nonlinear dynamics has opened up a host of new challenges for statistical physics. These challenges focus on characterizing, predicting and controlling the evolution of complex nonlinear processes in space and time. The statistical nature of the problem stems from the possibly intricate, hierarchical and fractal nature of trajectories in nonlinear dynamical systems, and the concomitant extreme sensitivity of the solutions to initial conditions, variation of parameters and system energy.

Here we will mainly investigate hamiltonian (energy-conserving) dynamical systems that exhibit such rich and varied behaviour, particularly looking at problems which were previously overshadowed or unknown. Although it is difficult to predict what will be the future central problem in chaotic dynamics, it is safe to select particle and field kinetics as providing a foundation for problems of importance. An ultimate goal is a kinetic description of chaotic dynamics which will generate insights into the nature of associated random processes (especially random walks), and their link to the theory of dynamical systems. Some aspects of kinetics in hamiltonian systems with chaos will be discussed below in detail. As we will show, simple nonlinearities in the hamiltonian can induce fractal motions with nonstandard statistical properties. We term such behaviour 'strange kinetics'.

Real orbits in dynamical systems are always theoretically predictable because they represent solutions of simple system of equations (for example Newton's equations). Under conditions for dynamical chaos, however, these orbits are highly unstable. Generally for chaotic motion the distance between two initially close orbits grows exponentially with time as

$$d(t) = d(0)\exp(\sigma t) \tag{1}$$

where the rate σ is called a Lyapunov exponent. This dependence holds for sufficiently long times. Local instabilities, described by equation (1), lead to a rapid mixing of orbits within the time interval $\tau_\sigma = 1/\sigma$. Nevertheless, some properties of the system remain fairly stable and their evolution occurs at a significantly longer timescale $\tau_D \gg \tau_\sigma$ as a result of averaging (possibly only partially) over the fast process of mixing, caused by the instability in equation (1). Kinetic equations arise as a consequence of such averaging. The well-known gaussian and poissonian statistics (for diffusion in space and temporal measures, respectively) can under certain conditions give a valid, albeit approximate, description of the apparent randomness of chaotic orbits. It has been realized, however, that behaviours much more complex than standard diffusion can occur in dynamical hamiltonian chaos. For hamiltonian chaos we will emphasize parameter regimes where Lévy statistics (describing fractal processes) apply and strange kinetics rules. Lévy statistics can appear both in space and time, and the fractal processes they describe lie at the heart of complex processes such as turbulent diffusion, chaotic phase diffusion in Josephson junctions, and slow relaxation in glassy materials.

Lévy statistics can be generated by random processes that are scale-invariant. This means that a trajectory will possess many scales, but no one scale will be characteristic and dominate the process. Geometrically, this implies the fractal property that a trajectory, viewed at different resolutions, will look self-similar. One example of a scale-invariant random process is a random walk with infinite mean-squared jump distances $\langle R^2 \rangle$ (the second moment of the jump distance probability, $p(R)$). A finite second moment would set a scale and lead to gaussian behaviour. The scale-invariant random walk is equivalent to studying the addition of random variables with infinite moments. Early examples of scale invariance were treated as paradoxes (see Box 1), but the general mathematics for determining probability distributions for the addition of random variables with infinite moments were developed by Paul Lévy in the 1920s and 1930s. Lévy's study of random processes with $\langle R^2 \rangle = \infty$ did not readily find physical applications because measurements of time-dependent relationships were generally required, of the form

$$\langle R^2(t) \rangle \sim t^\gamma \tag{2}$$

where t is time and γ is a constant. Lévy's ideas at first did not seem to address such problems, as time does not enter explicitly into the original Lévy process. To make the connection, one must take into account the time to complete a jump of the random walk. Strange kinetics for chaotic hamiltonian systems fall outside the domain of brownian motion, and their statistical nature is reflected by values of γ between unity (brownian motion) and two (ballistic motion). Turbulent diffusion, in an open system where energy is pumped in through mixing, is characterized by the value of $\gamma = 3$.

Here we explore stochastics and dynamics leading to equation (2) and tie both worlds together through the common thread of

BOX 1 The St Petersburg paradox

THIS classic paradox provides us with a beautiful example of a kind of scaling. The problem involves a game of chance. The game is to flip a coin until a head appears. There is a probability of $\frac{1}{2}$ that this occurs on the first flip, and a probability of $1/2^n$ that the first head appears on the nth flip. Suppose you win 2^n coins if $n-1$ tails occur before the first head. Then your expected winnings are $(1\times\frac{1}{2})+(2\times\frac{1}{4})+\cdots+(2^n/2^{n+1})+\cdots=\infty$. This game was introduced by Nicolaas Bernouilli (the nephew of Jacob and John) in the early 1700s, and is known as the St Petersburg paradox because Daniel Bernouilli wrote about it in the Commentary of the St Petersburg Academy. The question is how many coins a player has to risk (the ante) to play. Ideally, in a fair game, the ante should be to equal the expected winnings. The banker requires the player to ante an infinite number of coins because this is his expected loss. The player, however, favours a small ante because he will only win one coin half of the time, two coins or fewer with probability $\frac{3}{4}$, four coins or fewer with probability $\frac{7}{8}$, and so on. The two parties cannot come to an agreement because they are trying to determine a characteristic scale from a distribution which does not possess one. An infinite number of possible scales of winning (in powers of two) enter, but no scale is dominant. The discovery of this paradox was to cast doubt on the firm mathematical foundations of probability theory. Today, we see this paradox as a rich example of scaling with all its inherent exponents, fractal dimensions, and renormalization scaling properties.

fractal trajectories. First we discuss briefly the problem of a kinetic description of dynamical systems with chaotic behaviour, and mention some important topological properties of the phase portrait of the system. Then, within the context of the history of probability theory, we describe random processes (Lévy flights and Lévy walks) that are relevant to dynamical systems whose orbits possess fractal properties. We consider several examples of dynamical systems with 'symptoms' of Lévy-like processes. Finally we present a phenomenology of a kinetic description of dynamical systems undergoing chaotic motion ('strange kinetics') with fractal properties.

From chaotic dynamics to strange kinetics

An early step to describe kinetics in hamiltonian systems was the introduction of the Fokker–Planck–Kolmogorov (FPK) equation (or its equivalent). It seemed suitable as a natural tool for the description of the slow evolution of system variables[1]. The reason for this can be qualitatively explained by considering the 'standard map' of Chirikov-Taylor[2]. This map is obtained when considering the periodically kicked rotor

$$p_{n+1} = p_n + K_0 \sin x_n, \qquad x_{n+1} = x_n + p_{n+1} \tag{3}$$

where p and x are rotational momentum and phase of the rotor and n corresponds to the n-th instance of a kick, so n plays a role of discrete time. After each kick the rotor's momentum changes by $\Delta p = p_{n+1} - p_n$, which is proportional to the amplitude K_0, of the kick, and the changing of phase $\Delta x = x_{n+1} - x_n$. The map of equation (3) is typical of many physical problems and models many features of the occurrence of chaos. If $K_0 \gg 1$, then phase x, taken always in the interval $(0, 2\pi)$, changes randomly. Averaging over the phase, one can get easily from equation (3) the moments $\langle\langle \Delta p \rangle\rangle = 0$, $\langle\langle (\Delta p)^2 \rangle\rangle = K_0^2/2$ where $\langle\langle \cdot \rangle\rangle$ means averaging over x in the interval $(0, 2\pi)$. These simple expressions lead eventually to the diffusion (FPK) equation

$$\frac{\partial F(p)}{\partial t} = \frac{1}{2} D \frac{\partial^2 F(p)}{\partial p^2}, \qquad D = \langle\langle (\Delta p)^2 \rangle\rangle = K_0^2/2 \tag{4}$$

which describes the slow evolution of the momentum distribution function $F(p)$. This is the simplest manner in which a kinetic description arises in a dynamical system with chaotic behaviour. It is due to the randomness of the fast variable phase, generated by nonrandom equations such as (3) above.

Realistic physical systems appear to be more peculiar because of the inhomogeneity of their phase space where regions of both chaotic dynamics and regular (or quasiperiodic) dynamics are present. This phenomenon is often referred to as a 'stochastic sea' with 'islands' of stable nonrandom orbits (see Fig. 1 with explanations). The existence of such islands and their borders alters the pattern of diffusion dynamics, and early studies led to a different expression from that of equation (4) for the diffusion coefficient D (ref. 3).

$$D = K_0^2/2\{1 - 2J_2(K_0)\}$$

where J_2 is a Bessel function. The cause of the change in the $D(K_0)$ dependence is more important than the change itself: it arose from the discovery of a new topological object in phase space[4–6] which Percival called a cantorus. A cantorus can be imagined as a closed curve except for an infinite number of gaps, immersed in the stochastic sea. The gaps have different sizes so that the measure of the cantorus is zero (therefore a cantorus is fractal, rather than a typical curve which has the measure one). All points of a cantorus belong to the only orbit if the initial condition has been chosen from the cantorus manifold. Motion along cantori is periodic and unstable. Every island or set of islands (see Fig. 1) is enclosed with an infinite set of cantori.

The discovery of cantori changed the understanding of phase space structure and the transport within it. Particle transport takes place within the area of the stochastic sea and corresponds to a wandering amidst the islands. The wandering particle can pass through the gaps of cantori, which creates effective barriers for diffusion. The cantori closest to the island boundaries seem to be the most important, because their barriers are the widest and their gaps are the narrowest. The passage through the intervals between the islands is complicated by the fact that the nearest cantorus blocks the escape of the particle from the boundary layer in the vicinity of the island. The particle gets trapped inside the area between the island border and the nearest cantorus (or cantori) and this is the reason why one can observe higher densities of dots in the stochastic sea of Fig. 1. We cannot see cantori in Fig. 1, but they disclose themselves as boundaries of dark strips inside the stochastic sea domain.

This tendency to get trapped has been called 'stickiness', and it is the existence of 'sticky' orbits that makes the kinetics of the particle strange. Let us describe this in more detail. Consider a particle wandering in the stochastic sea area which passes through a gap of a cantorus very close to an island boundary. The particle now experiences a new kind of motion and almost regularly rotates around the island or around a set of islands. The rate of instability (Lyapunov exponent) near the island's boundary is small, so the motion is close to a quasiperiodic one. In addition, this cantorus (or cantori) blocks the possibility of escaping from the boundary layer area. As a whole it works as a trap for the particle. Thus trapping of the particle in the (x, p) plane corresponds to a 'flight' along the curve A_1A_5 in Fig. 1. In the multidimensional case, flight can be perpendicular to the (x, p) plane direction. In other words, trappings and flights are complementary features of anomalous excursions of the

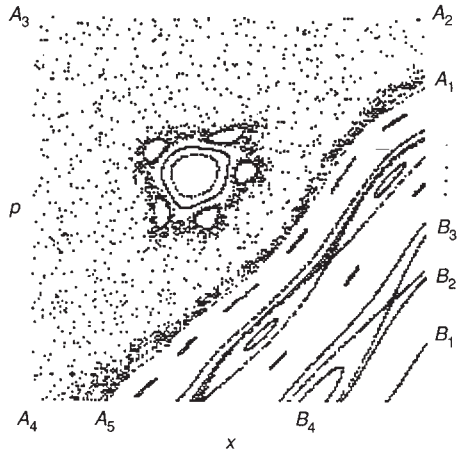

FIG. 1 Illustration of the topology of dynamical system orbits in the phase space (x, p). Starting from some initial conditions, the orbit is generated by an infinite set of iterations, equation (2), and each iteration gives a dot on the (x, p) plane. Such a procedure is called a Poincaré section. Instead of a continuous curve, the orbit is represented on the (x, p) plane by the set of values (x_n, p_n) taken at special set of time instants. We plot a typical part of the (x, p) plane for equation (2) with $K_0 = 1.2$. The regular orbits $(B_1, B_2, B_3, B_4, \ldots)$ describe quasiperiodic motion. In contrast to them, there is an orbit which fills the domain $A \equiv (A_1, A_2, A_3, A_4, A_5)$ (except for some area in its central part). There is no possibility of fitting all of these points onto one curve. This orbit represents chaotic motion. The area A is a 'stochastic sea'. Inside A there is a set of 'islands' in which the motion is regular. Domain A borders a big island along the curve A_5A_1 (there is only a part of the island in the figure and the orbits $B_1, B_2, \ldots$ are closed in this island). The density of points in the 'stochastic sea' area (or distribution function) displays how often this part of the phase space has been visited. The density is inhomogeneous and the most visited parts are narrow strips close to island boundaries. Dark strips of high density points are distributed along the border (A_1A_5) of the big island, around the smaller island and its five satellite sub-islands.

random-walk particle orbit. Such behaviour is not new in physics. In the theory of turbulence it is known as intermittency, and there are many examples of intermittent behaviour of dissipative dynamical system[7]; as well as of hamiltonian systems[8]. Actually the analogy with turbulence may be even deeper as will be seen later.

The crucial questions are what the probabilities are of anomalous orbits with strong intermittent dynamics, or how often one chaotic orbit will happen to exhibit intermittent bursts. It seems that the ability of dynamical chaos to have anomalous statistical properties is general, although sometimes it is difficult to observe. There are many examples of anomalous kinetics of particles due to flights and trappings: simulations of passive scalar dynamics in fluids[9–11], charged particle multidimensional dynamics[12], particle dynamics in two-dimensional periodical and quasiperiodical potentials[13,14], and experiments on transport in the presence of convective cells[15] or in the presence of regular patterned capillary waves[16]. Correspondingly, for flight observations there is evidence of anomalous diffusion of particles, so that in the expression for particle displacement R after time t (averaged over a number of orbits)

$$\langle |R| \rangle \sim t^{\mu} \qquad (t \leftarrow \infty) \tag{5}$$

the exponent $\mu \neq \frac{1}{2}$, which would be the value for normal diffusion (we are using the form of equation (5) instead of equation (2) for convenience). Sometimes μ can be close to one, corresponding to enormously strong enhancement of the transport ('ballistic motion'). Applications of this phenomenon include plasma fusion and understanding the spread of environmental pollution.

It seems now that the 'strange kinetics' described above are similar to the 'Lévy process'[17] which appeared as an alternative to the gaussian law of large numbers or the usual brownian motion. It is worth giving this story separately because it helps when trying to understand its deep relationship to dynamical chaos.

From St Petersburg to strange kinetics

We have mentioned that the complexity of chaotic orbits near the boundaries of islands resides in their self-similar behaviour on a small scale. To reflect such a property one cannot use a correlation length or a characteristic size. One has to introduce many scales, expecting a self-similarity among all of them. The history of probability theory has already provided us with an example of this type of scaling.

An example of random walk, formulated in the eighteenth century and known now as the St Petersburg paradox, has shown the existence of infinite moments (Box 1). Lévy generalized[17] the central-limit theorem to take such possibilities into account. He considered the distribution of sums of random variables with infinite moments. Let us add up several identically distributed random variables X_i. The value of each variable X_i can be thought of as a step in a random walk. Each jump length is chosen from a distribution $p(x)$. Lévy asked when the distribution of the sum of n steps $p_n(x)$ (up to some scale factors) would be the same as the distribution of any term in the sum, $p(x)$. This is basically the question of fractals: when does the whole (the sum) look like one of its parts? One answer to this question is well known: a sum of gaussians is a gaussian. The distribution of the X_i is $p(x) = (2\pi)^{-1/2} \exp(-x^2/2)$, the distribution of $p_n(x)$, the properly scaled sum $(n)^{-1/2} \sum_i X_i$ is $(2\pi n)^{-1/2} \exp(-x^2/2n)$. So $p(x)$ and $p_n(x)$ have the same distribution up the scale factor n. In Fourier space $(x \rightarrow k)$ $p_n(k)$ has a simple form

$$p_n(k) = \int_{-\infty}^{\infty} p_n(x) \exp(ikx)\, dx = \exp(-nk^2/2) \tag{6}$$

Note that the second moment of $p_n(x)$ is given by $-\partial^2 p_n(k=0)/\partial k^2 = n$. Lévy discovered that other solutions existed such that $p_n(x)$ and $p(x)$ had the same distribution. He found this to be the case when

$$p_n(k) = \exp(-\text{constant} \times n|k|^{\alpha}) \qquad (\text{for } 0 < \alpha \leqslant 2) \tag{7}$$

The $\alpha = 2$ case is the gaussian which we have just studied. For $\alpha < 2$, we note that $\langle x^2 \rangle = -\partial^2 p_n(k=0)/\partial k^2$ is infinite. These random walks with steps with infinite second moments are known as Lévy flights. It now seems obvious that to have scale-invariant distributions, we would need to sum up random variables with no scale. Indeed, applying an inverse Fourier transform to equation (7) gives

$$p_n(x) \sim \text{constant} \times n/x^{1+\alpha} \tag{8}$$

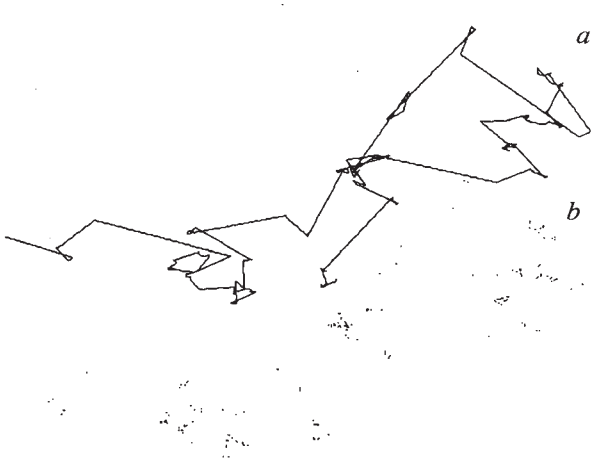

FIG. 2 The connected lines *a* show the trajectory of a Lévy walk. The isolated dots *b* show the points visited by a Lévy flight which represents the turning points of the Lévy walk in *a*. The trafectory is plotted from a two-dimensional version of equation (*) in Box 2 with $\alpha = \ln 2/\ln 3$. Number of points is 350.

BOX 2 Weierstrass random walks

To obtain a deeper understanding of the new kind of the characteristic function $p(k)$ in equation (7) in the text, consider a special example of random walk which can be written in the form

$$p_w(x) = \frac{\alpha - 1}{2a} \sum_{j=0}^{\infty} a^{-j}(\delta_{x+b^j} + \delta_{x-b^j}) \tag{*}$$

where δ_{xy} means the Kronecker symbol. Jumps of size $\pm 1, \pm b, \pm b^2$ and so on can occur, but jumps an order of magnitude longer in base b occur an order of magnitude less often in base a. We make about a jumps of length unity before, on the average, a jump of length b occurs, and so on, until in a hierarchical fashion patchy clusters of all sizes are formed. Taking the Fourier transform of $p_w(x)$, we arrive at

$$p_w(k) = \frac{a-1}{a} \sum_{j=0}^{\infty} a^{-j} \cos(b^j k)$$

which is the Weierstrass function. The important part of this result is that the random walk process (*) describes a situation that reflects the scaling of the St Petersburg paradox. This process is related to the Weierstrass function which possesses the scaling property:

$$p_w(k) = a^{-1} p_w(bk) + \left[\frac{a-1}{a}\right] \cos(k)$$

The detailed analysis of this equation[19,43] gives the final result in the form

$$p_w(k) \sim 1 - |k|^{\alpha} \sim \exp(-|k|^{\alpha})$$

with $\alpha = \ln a/\ln b$ when $b^2 > a$ so $\langle x^2 \rangle$ is infinite. Value α represents the fractal dimension of a random walk path[18,19,43]. This exponential form with the fractional power comprises the non-gaussian solution to Lévy's question addressed in equation (7). If one wants to add random variables (take a random walk) and have the probability distribution after n steps look like the probability distribution after one step (except for a change of scale), then your random variables are either gaussian or have infinite second moments. This means the solution is either gaussian or fractal. The process $p_w(x)$ is used to illustrate Lévy flights in Fig. 2.

where the power law for the tail of the distribution indicates the absence of a characteristic size unlike the gaussian distribution, where $\alpha = 2$. We emphasize that sums governed by equation (8) with $\alpha < 2$ are dominated by their largest terms, and thus by rare intermittent events. It can also be seen from equation (8) that the power-law behaviour of the tail of the distribution function defines the appreciable probability of large values of displacement x, explaining the reason for 'Lévy flights'. The exponent α will turn out to be the dimension of the point set visited by a Lévy flight. For Lévy flights this dimension is fractal ($0 < \alpha < 2$). Mandelbrot has connected the fractal properties of random walks with Lévy flights[18] (see also ref. 19). This may be important especially for turbulence problems, discussed below.

A non-poissonian distribution is the forerunner of the concept of fractal time where the waiting times between jumps occur on all scales, but with order of magnitude longer waits occurring an order of magnitude less often. For fractal time the average, $\langle t \rangle$, between events is infinite. This does not mean that the duration between every event is infinite, just as in the coin game of the St Petersburg paradox not every player wins an infinite amount of money just because the expected winning is infinite.

It is not so difficult now to introduce fractal time[20,21] into random walks. In some sense it could be done in a similar manner to the fractal space random walk. Indeed, let the time sequence $t_0, t_1, \ldots \equiv \{t_j\}$ be the sequence of moments when steps of the random walk are performed. Formally there are no restrictions on the structure of the $\{t_j\}$, especially in a dynamical system and $\{t_j\}$ is (for example) a set of crossing times of the Poincaré section. A more detailed description is based on the introduction of a time delay function $\psi(t)$ which is the probability density that the duration between events is t. The behaviour of $\psi(t)$ may be similar to the scaling of the Weierstrass function (Box 2). As will be seen later, the combination of fractal time and space for random walks can create essentially a new kind of wandering which is the background of strange kinetics.

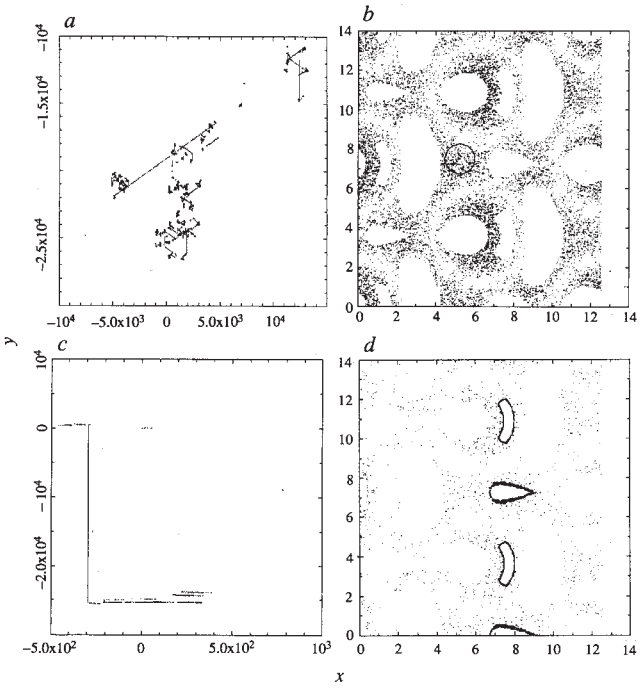

FIG. 3 Poincaré section of a streamline (or passive particle) with $\varepsilon = 2.3$ (ref. 42). Each dot represents a crossing of the streamline (or particle orbit) with the plane $z = 0$ (mod 2π). This corresponds to anomalous transport with $\mu > \frac{1}{2}$ (see Fig. 4). *a*, A general impression of the particle's wandering. There are many tracks which represent flights. Some of them have length of order 10^4. *b*, Small-scale plot of the same orbit. The area is of order $4\pi \times 4\pi$. They are a part of the stochastic web and many islands. The full stochastic web can be obtained from *b* by its periodic continuation in x and y directions. *c*, A special part of the orbit which corresponds to an initial condition taken inside the circle in *b*. It is a very long flight of order of 10^4. If we plot all the points *c* onto the small square x (mod 4π), y (mod 4π) then we obtain a new visualization, *d*. Dark strips around some islands correspond to frequent visits to these areas by the particle; they result from trapping due to the stickiness of the islands' boundaries. This picture confirms that islands create the tracks for flights.

Lévy flights and walks

Our discussion has so far evolved from the observation that chaotic diffusion in dynamical systems can be shown by particle trajectories which are reminiscent of Lévy flights. (Evidence of this will be given in the next section). Beautiful and elegant as the mathematics of Lévy flights are, they are not directly applicable to the kinetic description of real dynamical processes. One must take into account the time to complete each jump of the random walk. This process we have named the Lévy walk[22]. One then looks at the displacement after a time t rather than an n steps. Even when the average jump distance is infinite (a Lévy flight) the average displacement after a time t (a Lévy walk) will be characterized by a time-dependent growth, such as t^{μ} in equation (5). Lévy walks are a modification of the flights, preserving the spatial self-similarity. To overcome the divergence in $\langle R^2 \rangle$, a time cost is introduced so that long steps are penalized. The formulation of Lévy walks rests on a continuous time random walk (CTRW) approach. The nature of the walks is entirely specified by the probability distribution $\Psi(r, t)$ for a single step of $\mathbf{r}$ in time t. This probability density has the following property.

$$\int d\mathbf{r}\, dt\, \Psi(\mathbf{r}, t) = 1, \qquad \Psi(\mathbf{r}, t) = p(r)\delta(t - |\mathbf{r}|/v(\mathbf{r})), \qquad p(\mathbf{r}) \underset{r\to\infty}{\sim} |\mathbf{r}|^{-\mu} \tag{9}$$

The second property relates the step length to time in terms of a length-dependent velocity. This space–time coupling is mathematically essential to avoid the divergences of Lévy flights. The third property is responsible for the self-similarity of trajectories and by itself represents the Lévy flight. The 'secret' in getting rid of the divergence typical of the flight's mean-square displacement lies in the space–time coupling of $\Psi(\mathbf{r}, t)$ through the δ-function. Space–time fractal behaviour is introduced directly through coupling on $\Psi(\mathbf{r}, t)$. Figure 2 shows a two-dimensional realization of a Lévy walk where $v(\mathbf{r}) = \text{constant}$ and the fractal dimension is $\ln 2/\ln 3$. The self-similar aspect of the picture is important: a series of small steps is followed by larger ones, which are then followed by larger ones still; furthermore, no particular length scale dominates. These features of the Lévy walk make them attractive in simulating momentum mixing over large distances, and they are therefore candidates for turbulent diffusion and turbulent flows[23]. In fact, Hayot[24] was able to take advantage of this picture and calculate the velocity profile for inertial range turbulent pipe flow, and turbulent flow past a cylinder.

Phase rotation in Josephson junctions provides an example of a Lévy walk. For a constant voltage across a junction, the phase difference between current and voltage will rotate at a constant rate. Under certain conditions, however, involving the amplitude of a driving force, the phase can switch back and forth intermittently between clockwise and counterclockwise rotations[25–27]. One can consider the distribution of times spent in a given rotation state. If the phase rotates n times in the clockwise sense we consider this as a step of length n to the right in a one-dimensional random walk. The junction can be operated such that the distribution $p(n)$ for having n consecutive rotations in the same direction will be a Lévy distribution possessing an infinite second moment. But the mean value of $\langle x^2(t) \rangle$, where x is the phase difference, will not be infinite. This

is because each rotation takes a finite time to be completed, so by time t only a finite number of rotations can occur. The scaling of the mean squared displacement $\langle x^2(t)\rangle$ is a function of time and can exhibit the accelerated behaviour $\langle x^2(t)\rangle = t^\mu$ with $1 < \mu \leqslant 2$ (ref. 26).

Even more accelerated motion is possible and the law $\langle R^2(t)\rangle \sim t^3$ is well known for turbulent diffusion, as Richardson's law. For the random walk corresponding to the Josephson junction example, flight paths were traversed with a constant velocity. A Lévy set of trajectories where the velocity depends on the flight length will reproduce Richardson's law[22] when the $v(\mathbf{r})$ in equation (10) is given by $v(\mathbf{r}) = |\mathbf{r}|^{1/3}$, and $p(\mathbf{r})$ describes a Lévy flight. This $v(\mathbf{r})$ relation is the signature of Kolmogorov's scaling for inertial range of turbulence. It represents particle trajectories encountering a hierarchy of larger and larger vortices as time progresses. The Lévy walk approach not only arrives at the proper scaling law, but in addition gives a Lagrangian description of particle trajectories. Modifications to Richardson's law have also been investigated in the framework of random walks[22,23].

Patterns, stochastic webs and strange kinetics

We now discuss several dynamical models for which the phenomena of anomalous, non-gaussian transport (see equation (5)) with $\mu \neq \frac{1}{2}$ have been observed. The models describe hamiltonian systems for which the Liouville theorem (of the preservation of phase volume) is relevant. This means that the initial area in the phase, bounded by a surface, can change its form drastically, but the volume surrounded by the surface cannot change. The crucial feature of this treatment is to show how the existence of flights (or trappings) and anomalous kinetics is connected to symmetry properties of a system or, more generally speaking, to a symmetry of the system's phase portrait in phase space[25-29].

As the first example let us consider the 'Q-flow'[28] defined as

$$\mathbf{v} = (\partial\psi_q/\partial y + \varepsilon \sin z, -\partial\psi_q/\partial x + \varepsilon \cos z, \psi_q) \qquad (10)$$

where ε is a parameter. Here the generating symmetry function ψ_q is

$$\psi_q = \sum_{j=1}^{q} \cos(\mathbf{R}\cdot\mathbf{e}_j), \qquad \mathbf{R} = (x, y)$$
$$\mathbf{e}_j = (\cos 2\pi j/q, \sin 2\pi j(q)) \qquad (j = 1, \ldots, q) \qquad (11)$$

where q is the order of symmetry, and $\mathbf{e}_j$ is set of unit vectors, which form the regular star. Lines of constant ψ_q generate the q-fold symmetry pattern in the (x, y) plane, which is of crystal-like symmetry for $q \in q_c = \{1, 2, 3, 4, 6\}$ and is of quasicrystal-like symmetry for $q \notin q_c$. The Q-flow is incompressible ($\operatorname{div}\mathbf{v} = 0$) and of Beltrami type ($\mathbf{v} = \operatorname{curl}\mathbf{v}$), described in detail in ref. 29. The best known is the case of cubic symmetry flow when $q = 4$ and $\psi_4 = 2(\cos x + \cos y)$, the 'Arnold-Beltrami-Childress' (ABC) flow. Interest in the ABC flow has been raised by the nontrivial chaotic behaviour of the flow's streamlines[30-32] and by applications to the fast dynamo problem. It should be mentioned that any Q-flow has a stochastic web in real coordinate space[8,29], which means the following. The set of equations $dx/v_x = dy/v_y = dz/v_z$ defines the flow's streamlines. Its solution for v from equation (10) displays an infinite connected net of channels of finite width of order ε, inside which streamlines look like random contours, which leads one to conclude that passive scalar dynamics is diffusive. We will see later that the transport through the stochastic web is anomalous or 'strange' for general situations[9,10], implying the existence of flights and trappings, and also implying that $\mu \neq \frac{1}{2}$ in the asymptotic formula, equation (5).

Observations of flights for different models can be sketched as in Fig. 3. Flights (or trappings) appear along the island's boundary, and the existence of pattern symmetries is crucial for determining the probability of their occurrence. If the patterns are destroyed, the long flights and anomalous transport properties disappear. This is why the generation function ψ_q in equation (10) is of great importance. It possesses general symmetry properties and creates different directions of flights in the phase space and real space of Q-flow. In particular, changing the parameter ε in equation (10) changes some aspects of the phase portrait. The number of islands, their locations, sizes and shape all depend on ε. The levels of stickiness of the island boundary, and the cantori closest to them, are also functions of ε. This is revealed in the sensitive dependence of μ on ε. For $q = 6$ (hexagonal symmetric flow) the curve $\mu = \mu(\varepsilon)$ was obtained in ref. 9. (See Fig. 4) All variations of μ in the plot correlate one-to-one with sharp changes in the phase portrait of the system after ε has passed through some critical values. The influence of the closeness of ε to such a critical value was found[10] for the equations (10 and 11) with $q = 5$. Figure 5 explains how this could happen. For some intervals of ε there are special domains in the phase space of very long particle trapping which creates extremely long flights, called stochastic jets. The escape of any orbit from a bundle of orbits, initially inside the trapped chaotic area, is blocked by a cantorus. The scattering of the bundle is very small and the bundle survives as a long jet. The time of

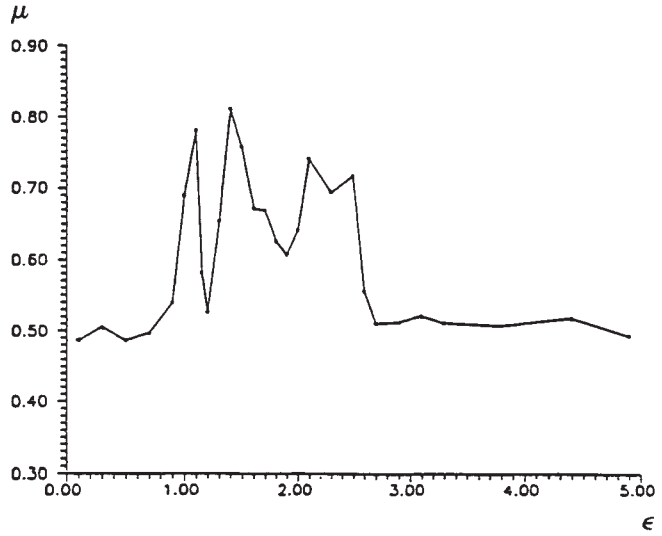

FIG. 4 The dependence of the diffusional exponent $\mu = \mu(\varepsilon)$ (ref. 9), for the same hexagonal flow as in Fig. 3. There is a region of ε between ~0.8 and 2.8 where μ fluctuates strongly between $\frac{1}{2}$ and 1.

survival of a jet can be comparable with any timescale of observation or simulation. Such jets imply that the exponent μ is close to one (ballistic behaviour).

Another model, for which flights, stochastic jets and anomalous transport were observed in detail[12] is the four-dimensional mapping

$$u' = [u + K\sin(v - z)]\cos\alpha_0 + v\sin\alpha_0$$
$$v' = -[u + K\sin(v - z)]\sin\alpha_0 + v\cos\alpha_0 \qquad (12)$$
$$p' = p + K_0\sin(v - z), \qquad z' = z + p'$$

Equations (12) describe particle motion in a magnetic field and in a wave packet which propagates obliquely to the magnetic field. Here u is a dimensionless velocity along x and v is the coordinate x; p and z are dimensionless velocity and coordinate along the magnetic field; α and K, K_0 are dimensionless parameters. The first two equations in (12) describe the so-called web-map which generates the stochastic web of the q-fold symmetry if $\alpha_0 = 2\pi/q$ with integer q. Averaging the hamiltonian for the first two equations in (12) will coincide with the pattern generator ψ_q in equation (11) if one puts $\vec{R} = (u, v)$. The second pair of equations in (12) coincides with the standard map, equation (3). Thus system (12) described coupling of the standard and web maps. It demonstrates a rich collection of different dynamical features. Even for small K and K_0 the diffusion can be fast and anomalous. This diffusion is faster than the Arnold diffusion. Figure 6 represents the two cases of diffusion when trappings and flights occur after a fairly small parameter change. As in previous cases, the system in equation (12) possesses a symmetry in its phase space, which generates flights of different forms.

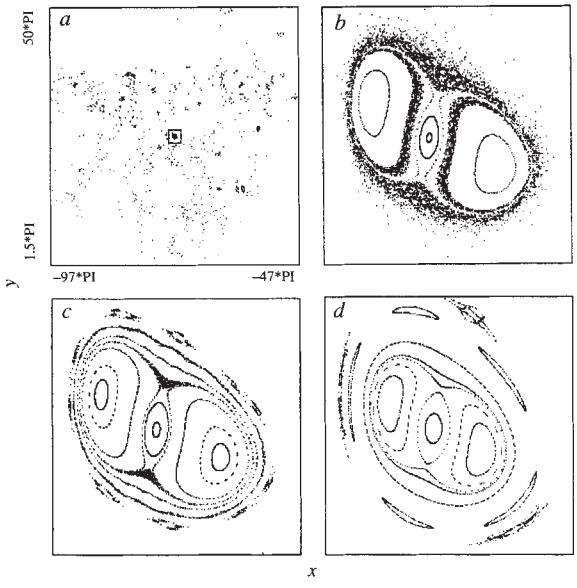

FIG. 5 The topological situation in phase space when extremely long flights, or trappings, occur[10]. We call them stochastic jets. All plots correspond to the 5-fold symmetry Q-flow ($q=5$ in equations (16) and (17)). Each plot is the (x, y)-coordinate of the only streamline when its z-coordinate value is $z=0$ (mod 2π). The case *a* plots long time transport for $\varepsilon=0.8$. Many black clusters of dots correspond to the streamline trapping in a small domain. Zooming into the small square in *a* gives *b*, which shows a figure '8'-like region with chaotic behaviour outside and inside the 8. These 'outer' and 'inner' areas of chaos are slightly connected (the white narrow strip does not absolutely separate them). This reflects small probability of penetration from the 'inner' chaotic area to the 'outer' one. If a particle has been trapped in the 'inner' area, it stays for a very long time which results in an appearance of jets in the perpendicular z-direction. Small variations of the parameter ε change the phase portrait of the system (*c* and *d*). In *c*, $\varepsilon=0.5$. A closed curve exists between 'inner' and narrow chaotic area and 'outer' one and the stochastic jets like in *b* have disappeared. The same is observed in *d*, where $\varepsilon=0.4$, and the 'inner' chaotic area is invisible. The existence or nonexistence of a low probability connection between 'inner' and 'outer' domains in *b*–*d* means that a wandering (outside the figure '8') particle can either be trapped for a long time in a small domain or cannot be trapped. This provides a micro-picture of the occurrence of superlong flights and trappings.

Clusters, multifractals and different length scales

An important observation[12] was the dependence of the diffusion exponent μ on the phase-space region where the set of initial coordinates is taken. This property reflects the inhomogeneity of μ for the same set of parameters (K, K_0, α). It is known that turbulent motion can be characterized by such inhomogeneous

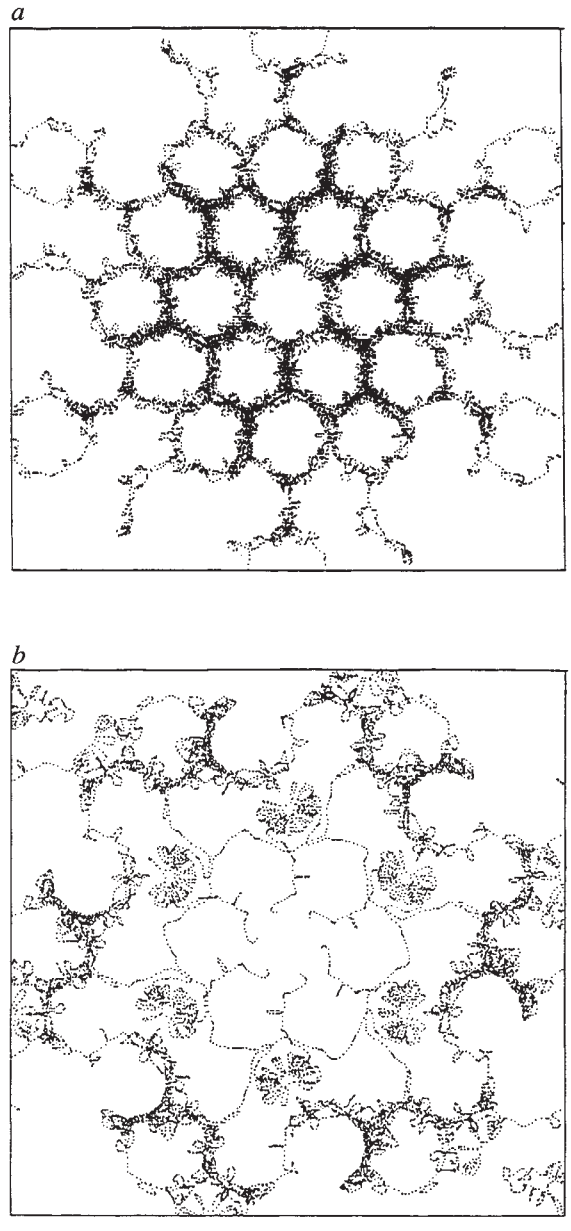

FIG. 6 The trajectory in *a* and *b* is part of a Lévy flight which does not possess any characteristic scale. If each segment is followed with a velocity proportional to the cube root of the segment length, then Richardson's law of turbulent diffusion ensues. Such trajectories can be used to simulate high Reynolds number fluid flows and are projections of particle's orbit onto the (u, v) plane for $\alpha_0=2\pi/6$ (hexagonal symmetry and $K=0.18$, for the model described by equations (18). In *a*, $K_0/K=0.3$ and diffusion through the stochastic web is close to the normal one. In *b*, $K_0/K=0.08$ and there are many flights along the web.

fractal properties[33]. One can imagine a fractal net or cluster imbedded into the real space, along which diffusion can occur. Now imagine several different nets or clusters imbedded into the same space. This provides a simplified representation of a multifractal: complicated, interpenetrating network of different fractals. In some sense, the same kind of idea is applicable to dynamical chaos. One can suppose the existence of local fractal dimensions in the phase space and clusters of different dimensionality. A particle diffusing along a cluster can switch from time to time to another cluster. If the measure of clusters with long flights is considerable, then their input to the diffusional exponent μ should be important. This, along with finite observation times and the choice of initial conditions, will define the final value μ

$$\mu = \mathcal{M}(\alpha, \beta; L, T) \tag{13}$$

where α and β are fractal exponents of local space and time singularities of the transition probability (see below); L and T are large-scale distance and time, and $\mathcal{M}$ is the corresponding functional. Let us mention that the usual definition of the diffusion constant from equation (3)

$$D = \lim_{\Delta t \to 0, \Delta x \to 0} \langle\langle (\Delta x)^2 \rangle\rangle / \Delta t = \text{constant} \tag{14}$$

gives the necessary connection (equation (13)) in the gaussian case ($\alpha = 1, \beta = 1$) for μ to be equal to $\beta/2\alpha = \frac{1}{2}$.

The cases of the kinetic descriptions in which the processes of flights and trappings are important have been broadly discussed[22], especially in the context of fractal space and fractal time. The generalization to the multifractal case is detailed in ref. 12, and the fractional Fokker–Planck–Kolmogorov (FFPK) equation was derived in ref. 34. It is beyond the scope of this article to discuss the FFPK equation and we present here only some of its features. One further consideration is to generalize the idea of diffusion constant. The basic idea involves performing the limit $\Delta t \to 0$, $\Delta x \to 0$ in equation (14). For homogeneous and smooth t and x processes, the procedure is straightforward. When this is not the case, the limit has many flights and trappings. On many scales we encounter the limit (see for example refs 35, 43)

$$\mathcal{B} = \lim_{\Delta t \to 0, \Delta x \to 0} |\Delta x|^{2\alpha} / |\Delta t|^{\beta} = \text{constant} \tag{15}$$

which replaces equation (14) and produces the scaling $x^2 \sim t^{\beta/\alpha}$. It is not a simple matter to obtain the unknown contants α and β from the properties of the phase space of a system because they should come from the analysis of fine details of the cantori described earlier. Nevertheless one can assume that invisible cantori are in charge of the local properties of the phase space and the limit (equation (15)) defines the large-scale properties of the transport process. It has been shown[12,34] that the constant μ in equations (5) and (13) is $\mu = \beta/2\alpha$, and that is the way in which fractal properties of space and time (fractal because α and β in equation (15) are fractional) allow us to deduce anomalous transport, connecting fractal space and time inherent in Lévy-like processes[19].

The above examples show that chaotic dynamics are related to the phenomena of Lévy flights and walks. One should expect, however, that different intermediate asymptotics could exist which correspond to normal diffusion as well as to anomalous transport with different exponents. Such a picture is consistent with the general multifractal property of chaos.

Scaling and strange kinetics have many applications to situations other than those discussed here: the physics of fluids, plasmas, macromolecules, computer sciences, chemical kinetics and technological problems[23,24,36–41]. The potential for strange kinetics exists in any situation where some hierarchical ordering of the random walk occurs. It happens in the random walk of electrons in disordered media (when localized states are of importance[21,36,40]), in the kinetics of macromolecules and in aggregation processes where a long-range correlation exists[38,39]. Problems of anomalous diffusion and anomalous conductivity in plasmas provide a good number of examples of kinetics with scaling[37]. We hope that a unified understanding of these examples could build a generalized approach for a kinetic theory of processes with long-time memory and long-range correlations as now exists for gaussian-like random dynamics. □

Michael F. Shlesinger is at the Physics Division, Office of Naval Research, 800 North Quincy Street, Arlington, Virginia 22217. George M. Zaslansky is at the Courant Institute of Mathematical Sciences and Physics Department, New York University, 251 Mercer Street, New York, New York 10012, USA. Joseph Klafter is at the Department of Chemistry, Massachusetts Institute of Technology, Cambridge, Massachusetts 02139 and School of Chemistry, Tel Aviv University: Ramat-Aviv, Israel 69978 (permanent address).

1. Zaslavsky, G. M. & Chirikov, B. V. *Uspekhi Fiz. nauk.* **105,** 3–39 (1971).
2. Chirikov, B. V. *Phys. Rep.* **52,** 264–379 (1979).
3. Rechester, A. B. & White, R. B. *Phys. Rev. Lett.* **44,** 1586–1589 (1980).
4. Percival, I. C. in *Nonlinear Dynamics and Beam–Beam Interaction* (eds Month, M. & Herrera, J. C.) Vol. 57, 302–310 (Am. Inst. Physics, New York, 1979).
5. Aubry, S. *Physica* D**7,** 240–258 (1983).
6. Mather, J. N. *Topology* **21,** 457–467 (1982).
7. Manneville, P. & Pomeau, Y. *Phys. Lett.* A**75,** 1–2 (1979).
8. Zaslavsky, G. M., Sagdeev, R. Z., Chernikov, A. A. & Usikov, D. A. *Weak Chaos and Quasiregular Patterns* (Cambridge Univ. Press, 1991).
9. Chernikov, A. A., Petrovichev, B. A., Rogalsky, A. V., Sagdeev, R. Z. & Zaslavsky, G. M. *Phys. Lett.* A**144,** 127–133, (1990).
10. Petrovichev, B. A., Rogalsky, A. V., Sagdeev, R. Z. & Zaslavsky, G. M. *Phys. Lett.* A**150,** 391–396 (1990).
11. Antonsen, T. M. & Ott, E. *Phys. Rev.* A**44,** 851–857 (1991).
12. Afanasiev, V. V., Sagdeev, R. Z. & Zaslavsky, G. M. *Chaos* **1,** 143–159 (1991).
13. Zaslavsky, G. M., Sagdeev, R. Z., Chaikovsky, D. K. & Chernikov, A. A. *Sov. Phys. JETP* **68,** 995–1000 (1989).
14. Chaikovsky, D. K. & Zaslavsky, G. M. *Chaos* **1,** 463–472 (1991).
15. Tabeling, P. & Cardoso, O. *Bull. Soc. fr. Phys.* **73,** 13–14 (1989).
16. Ramshankar, R., Berlin, D. & Gollub, J. P. *Physics Fluids* A**2,** 1955–1965 (1990).
17. Lévy, P. *Theorie de l'Addition des Variables Aleatoires* (Gauthier-Villiers, Paris, 1937).
18. Mandelbrot, B. *The Fractal Geometry of Nature* (Freeman, San Francisco, 1982).
19. Montroll, E. & Shlesinger, M. in: *Studies in Statistical Mechanics,* Vol. 11 (eds Leibowitz, J. & Montroll, E.) 1–121 (North-Holland, Amsterdam, 1984).
20. Shlesinger, M. F. *A. Rev. Phys. Chem.* **39,** 269–290 (1988).
21. Scher, H., Shlesinger, M. F. & Bendler, J. T. *Physics Today* **1,** 26–34 (1991).
22. Shlesinger, M. F., West, B. J. & Klafter, J. *Phys. Rev. Lett.* **58,** 1100–1103 (1987).
23. Viecelli, J. A. *Phys. Fluids* A**2,** 2036–2045 (1990).
24. Hayot, F. *Phys. Rev.* A**43,** 806–810 (1991).
25. Huberman, B. A., Crutchfield, J. P. & Packard, N. H. *Appl. Phys. Lett.* **37,** 750–752 (1980).
26. Geisel, T., Nierwetberg, J. & Zacherl, A. *Phys. Rev. Lett.* **54,** 616–619 (1985).
27. Ben-Jacob, E., Braiman, Y., Shainsky, R. & Imry, Y. *Appl. Phys. Lett.* **38,** 822–824 (1981).
28. Zaslavsky, G. M., Sagdeev, R. Z. & Chernikov, A. A. *Sov. Phys. JETP* **67,** 270–277 (1988).
29. Beloshapkin, V. V. *et al.* Nature **337,** 133–137 (1989).
30. Arnold, V. I. *C.r. hebd. Séanc. Acad. Sci., Paris* **261,** 17–20 (1965).
31. Henon, M. *C.r. hebd. Séanc. Acad. Sci., Paris* **262,** 312–314 (1966).
32. Dombre, T. *et al. J. Fluid Mech.* **159,** 353–391 (1983).
33. Frish, U. & Orszag, S. *Physics Today* **43**(1), 24–32 (1990).
34. Zaslavsky, G. M. in *Topological Aspects of the Dynamics of Fluids and Plasmas* (eds Moffat, H. K., Zaslavsky, G. M. Tabor, M. & Compte, P.) 481–491 (Kluwer, Dordrecht, 1992).
35. Gelfand, I. M. & Shilov, G. E. *Generalized Functions* Vol. 1 (Fizmat, Moscow, 1958). (Engl. transl.: Academic, New York, 1964).
36. Bouchaud, J.-P. & Georges, A. *Phys. Rep.* **195,** 127–293 (1990).
37. Isichenko, M. *Rev. mod. Phys.* **64,** 961–1044 (1992).
38. Havlin, S. & Ben-Avraham, D. *Adv. Phys.* **36,** 695 (1987).
39. Douglas, J. *Macromolecules* **22,** 1786–1797 (1989).
40. Blumen, A., Klafter, J. & Zumofen, G. in *Spectroscopy of Glasses* Vol. 1 (ed. Zschokke, I.) 199–265 (Reidel, Dordrecht, 1986).
41. Geisel, T., Zacherl, A. & Radons, G. *Z. Phys.* B**71,** 117–127 (1988).
42. Zaslavsky, G. M. & Tippett, M. K. *Phys. Rev. Lett.* **67,** 3251–3254 (1991).
43. Hughes, B. D., Montroll, E. W. & Shlesinger, M. F. *Proc. natn. Acad. Sci. USA* **78,** 3287–3291 (1981).

ACKNOWLEDGEMENTS. G.M.Z. thanks D. Stevens for help in preparing figures and the US Department of Energy for financial support. J.K. thanks R. Silbey for his hospitality at the Massachusetts Institute of Technology.